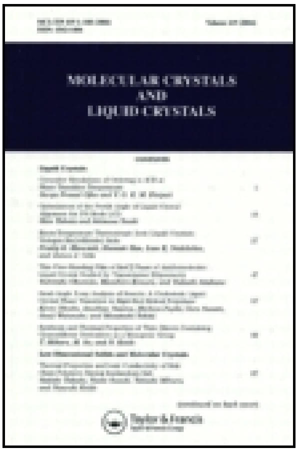

Molecular Crystals and Liquid Crystals Science and Technology. Section A. Molecular Crystals and Liquid Crystals
Publication details, including instructions for authors and subscription information:
http://www.tandfonline.com/loi/gmcl19

Magnetic Interactions in the Crystals of α- and β-Phases of 2-Hydro Nitronyl Nitroxide and Related Compounds

Yuko Hosokoshi [a] , Masafumi Tamura [a] , Kiyokazu Nozawa [a] , Satoshi Suzuki [a] , Hiroshi Sawa [a] , Reizo Kato [a] & Minoru Kinoshita [a]
[a] Institute for Solid State Physics, University of Tokyo, Roppongi, Minato-ku, Tokyo, 106, Japan

Version of record first published: 24 Sep 2006.

To cite this article: Yuko Hosokoshi , Masafumi Tamura , Kiyokazu Nozawa , Satoshi Suzuki , Hiroshi Sawa , Reizo Kato & Minoru Kinoshita (1995): Magnetic Interactions in the Crystals of α- and β-Phases of 2-Hydro Nitronyl Nitroxide and Related Compounds, Molecular Crystals and Liquid Crystals Science and Technology. Section A. Molecular Crystals and Liquid Crystals, 271:1, 115-122

To link to this article: http://dx.doi.org/10.1080/10587259508034044

Mol. Cryst. Liq. Cryst., 1995, Vol. 271, pp. 115–122
Reprints available directly from the publisher
Photocopying permitted by license only

MAGNETIC INTERACTIONS IN THE CRYSTALS OF α- and β-PHASES OF 2-HYDRO NITRONYL NITROXIDE AND RELATED COMPOUNDS

YUKO HOSOKOSHI, MASAFUMI TAMURA, KIYOKAZU NOZAWA, SATOSHI SUZUKI, HIROSHI SAWA, REIZO KATO, AND MINORU KINOSHITA
Institute for Solid State Physics, University of Tokyo, Roppongi, Minato-ku, Tokyo 106, Japan

Abstract Magnetic properties and crystal structures of α- and β-2-hydro nitronyl nitroxide radicals (2-hydro-4,4,5,5-tetramethyl-4,5-dihydro-1*H*-imidazol-1-oxyl 3-oxide) were investigated. Exchange couplings in both phases were estimated from the paramagnetic susceptibility (1.8–300 K) and magnetization (up to 400 kOe) measurements. Assignment of the couplings to molecular packings has been carried out. Close spacing between the ONCNO moieties yields various magnitude of exchange couplings from 0 to *ca.*–30 K. In α-phase crystal, short contacts between the central carbon atoms with negative spin density and the NO groups with positive spin density were observed. However, this packing is assigned to an antiferromagnetic exchange coupling, $J/k_B = -11$ K ($\mathcal{H} = -2J\boldsymbol{S}_1 \cdot \boldsymbol{S}_2$). This case suggests that care must be taken when we refer to McConnell's proposal.

INTRODUCTION

We have studied the magnetic properties of a series of substituted phenyl nitronyl nitroxide radical crystals since the discovery of the first purely organic ferromagnet[1,2] aiming to know the relation between the magnetic exchange couplings and the crystal structures. In these compounds, ferromagnetic or antiferromagnetic exchange couplings have been attributed to the interactions between the NO group and the phenyl ring or to the ones between the NO groups, respectively.[3–6] In nitronyl nitroxides, most of the spin densities are concentrated on the ONCNO moiety and the relative arrangement of this unit plays substantial role in magnetic interactions.

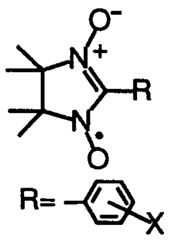

R=H,Br,I

In this paper, we report on the magnetic properties and crystal structures of α- and β-phases of 2-hydro nitronyl nitroxide radicals (2-hydro-4,4,5,5-tetramethyl 4,5-dihydro-1*H*-imidazol-1-oxyl 3-oxide, abbreviated as HNN). Replacing the phenyl ring by a monoatomic substituent, we expect direct interactions between the ONCNO moieties. Exchange couplings in both phases were estimated from the paramagnetic susceptibility (χ_p) and magnetization measurements. The relation between the exchange couplings and the molecular packings are discussed. Magnetic properties and crystal structures of 2-bromo and 2-iodo nitronyl nitroxide (abbreviated as BrNN and INN, respectively) are also presented.

EXPERIMENTAL

The radicals were synthesized by the reported path.[5,7] Single crystals were grown by slow evaporation of concentrated solutions. X-ray intensity data were collected by a MAC Science automated four-circle diffractometer at 298 K. Cell parameters are listed in Table IV. Magnetic susceptibilities (1.8–300 K) were measured by use of a Quantum Design MPMS SQUID magnetometer. For the estimation of the molar diamagnetic susceptibility (χ_d), we used cylindrical compaction samples (ϕ; 5mm, height; 2.2–2.8mm, weight; 63–72mg). The magnetization process was measured in pulsed magnetic fields up to 400 kOe (1.6–10 K).

RESULTS AND DISCUSSION

Crystal Structures of α- and β-HNN

HNN crystallizes in two different phases. Around 76 °C, an α-phase crystal undergoes structural phase transition to a β-phase crystal.

TABLE I Summary of crystallographic data with standard deviation in parentheses

	α-HNN	β-HNN	BrNN	INN
	$P2_1/n$	$P2_1$	*Pbca*	*Pbca*
a/Å	11.879(3)	19.991(4)	11.265(2)	11.454(3)
b/Å	11.611(2)	14.091(3)	16.851(3)	17.396(5)
c/Å	6.332(2)	12.144(2)	10.182(2)	10.069(3)
β/°	104.48(2)	92.92(2)	–	–
V/Å^3	845.6(3)	3416(1)	1932.8(5)	2006.3(9)
Z	4	16	8	8

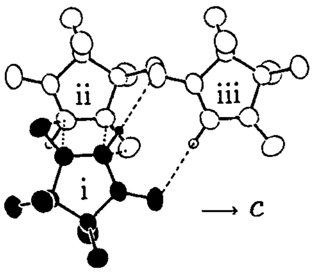

FIGURE 1 Crystal structure of α-HNN viewed along the direction perpendicular to the ONCNO plane of molecule i.

Figure 1 shows the molecular packing of α-HNN. Chains elongate along the c-axis. Each chain consists of two alternating packing modes corresponding to the inversion centers (mode A; i· · ·ii, mode B; i· · ·iii). O· · ·H distance (2.41(3) Å) and C-H-O angle (162(3)°) in mode B indicate the presence of weak hydrogen bonding.

Figure 2 (a) shows the molecular packing of β-HNN projected onto the bc-plane. Eight molecules drawn in Figure 2 (a) are crystallographically independent. Two packing modes similar to those in the α-phase crystal are observed. Figures 2 (b) and (c) represent the two packing modes; mode A consists of the close spacing between the NO groups and mode B consists of the one between the NO group and the CH group. The intermolecular atomic distances are listed in Table II.

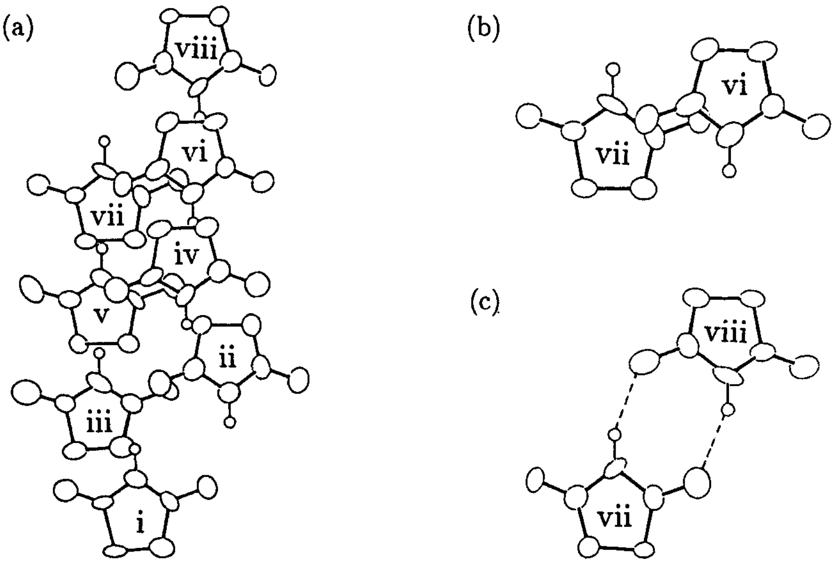

FIGURE 2 (a) Crystal structure of β-HNN projected onto the bc-plane. (b) Packing mode A viewed along the direction perpendicular to the ONCNO plane of molecule vi. (c) Packing mode B viewed along the direction perpendicular to the ONCNO plane of molecule viii.

TABLE II Intermolecular atomic distances (Å)

α-HNN						
mode A					mode B	
O···O	O···N	O···C	N···C	C···C	C···O	C···H
3.80	3.60	3.40	3.54	3.70	3.38	2.41

β-HNN					
	mode A			mode B	
$p\cdots q$	$N^p\cdots O^q$	$O^p\cdots N^q$	$p\cdots q$	$C^p\cdots O^q$	$O^p\cdots C^q$
vii···vi	3.82	4.20	vii···viii	3.13	3.09
v···iv	3.54	4.19	v···vi	3.22	3.13
iii···ii	5.11	4.81	iii···iv	3.33	3.16
i···viii	4.97	4.70	i···ii	3.17	3.14

Magnetic Properties of α- and β-HNN

χ_{d} of HNN was estimated to be $(-0.90 \pm 0.05) \times 10^{-4}$ emu mol^{-1}. This value can be used as a standard for other nitronyl nitroxide derivatives. Table III shows the comparison of the estimated χ_{d} values between HNN, BrNN, and INN. They are consistent with the ones calculated using the Pascal law.[8]

TABLE III Diamagnetic susceptibilities (χ_{d}) with errors in parentheses

	$\chi_{\mathrm{d}}/10^{-6}$emu mol^{-1}		radical
	calculated[a]	observed	content/%
HNN	−95	−90(5)	99(1)
BrNN	−120	−115(5)	99(1)
INN	−135	−135(5)	97(1)

[a] Calculated on the basis of the Pascal law.[8]

The temperature dependence of $\chi_{\mathrm{p}}T$, which is proportional to the square of the effective moments is shown in Figures 3 (a) and 4 (a) for α- and β-HNN, respectively. The $\chi_{\mathrm{p}}T$ values of α-HNN decreases monotonically with decreasing temperature. On the other hand, the $\chi_{\mathrm{p}}T$ against T plot for β-HNN exhibits stationary behavior around 10 K. The stationary value is about the half of the room temperature value.

Figures 3 (b) and 4 (b) shows the magnetization process at low temperature. The magnetization isotherms of α-HNN saturate around 200 kOe and each isotherm crosses around 160 kOe. The saturation value is corresponding to the parallel alignment of 1 mol of $S = 1/2$ spins. On the other hand, the magnetization isotherms of β-HNN at 1.6 and 4.2 K with the field range 150–300 kOe take a constant value corresponding to the parallel alignment of 1/2 mol of $S = 1/2$ spins. Above 300 kOe,

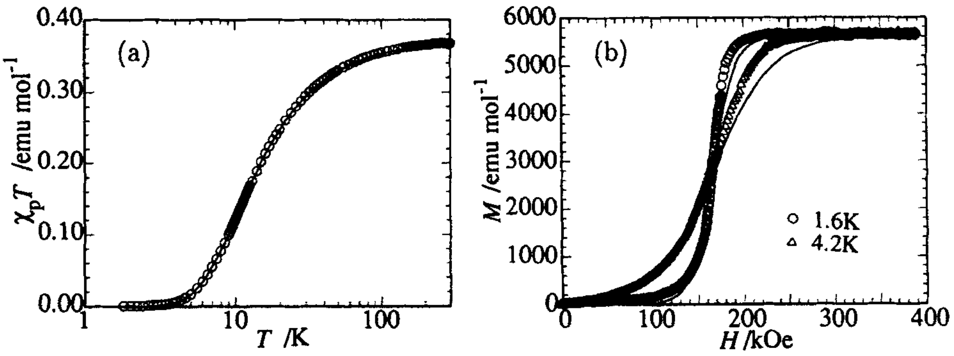

FIGURE 3 (a) Temperature dependence of χ_pT for α-HNN. (b)Magnetization process of α-HNN. Solid curves represent the fitting results by the dimer model with $J/k_B = -11$ K.

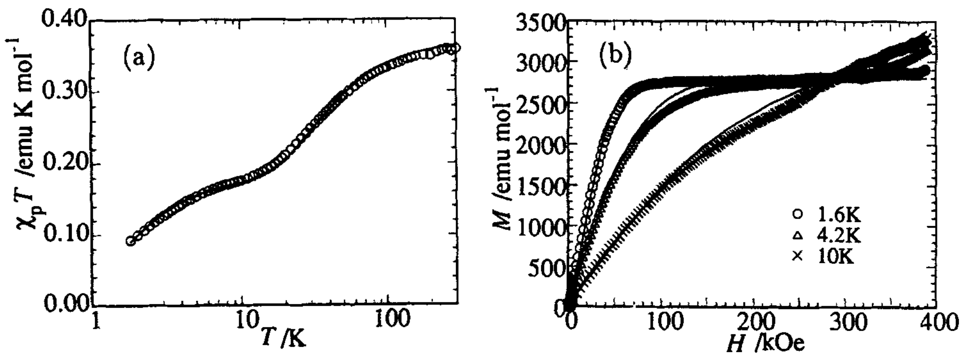

FIGURE 4 (a) Temperature dependence of χ_pT for β-HNN. (b)Magnetization process of β-HNN. Solid curves represent the fitting results by four independent dimers model (see text).

the beginning of the second saturation process is recognized.

Magneto-structural Correlation

Both of the χ_pT against T plot and magnetization curves of α-HNN in Figure 3 can be explained by the dimer model with $J/k_B = -11$ K ($\mathcal{H} = -2J\boldsymbol{S}_1 \cdot \boldsymbol{S}_2$). This indicates that only one of the modes (A or B) has antiferromagnetic coupling; the magnetic coupling in the other one is negligible. Then, which mode is responsible for the antiferromagnetic coupling? This question will be answered from the examination of β-HNN.

The most outstanding feature of β-HNN is the stationary behavior in the χ_pT against T plot and in the magnetization isotherms. This means that a half of the spins in the system are strongly coupled, while the rest are weakly coupled. Then, at least, two exchange couplings, J_1 and J_2 ($|J_1| \gg |J_2|$) are required to explain the magnetic behavior of β-HNN. According to Table V, the intermolecular geometries belonging to mode B are almost the same. On the other hand, those belonging to mode A comprise two categories; the atomic distances within the two pairs, vii $\cdots$ vi and v $\cdots$ iv, are appreciably shorter than the ones within the two pairs, iii $\cdots$ ii and i $\cdots$ viii. Therefore, it is natural to take each of the four dimers (vii $\cdots$ vi, v $\cdots$ iv, iii $\cdots$ ii, and i $\cdots$ viii) as a magnetic unit. We analysed both the $\chi_{\mathrm{p}}T$ against T plot and the magnetization isotherms of β-HNN in Figure 4 by four independent dimers model, $\mathcal{H} = -2J_1(\boldsymbol{S}_{\mathrm{vii}} \cdot \boldsymbol{S}_{\mathrm{vi}} + \boldsymbol{S}_{\mathrm{v}} \cdot \boldsymbol{S}_{\mathrm{iv}}) - 2J_2(\boldsymbol{S}_{\mathrm{iii}} \cdot \boldsymbol{S}_{\mathrm{ii}} + \boldsymbol{S}_{\mathrm{i}} \cdot \boldsymbol{S}_{\mathrm{viii}})$. Satisfactory fit was obtained using the parameters $J_1/k_{\mathrm{B}} = -33$ K and $J_2/k_{\mathrm{B}} = -1.5$ K. Since two dimers in each category (vii $\cdots$ vi and v $\cdots$ iv / iii $\cdots$ ii and i $\cdots$ viii) are not equivalent to each other, the estimated J_1 and J_2 values should be considered as average ones.

The exchange coupling, $J_1/k_{\mathrm{B}} = -33$ K is considerably large among those of neutral nitronyl nitroxides which we studied. In phenyl derivatives, interactions between the NO groups with N$\cdots$O distances of about 3.7 Å bring about antiferromagnetic couplings of $J/k_{\mathrm{B}} \approx -10$ K.[3,4] It should be noticed that sizable difference in the magnitude of exchange coupling is caused by slight change in intermolecular overlap.

Now, we return to α-HNN. Mode B in α-HNN resembles those in β-HNN. The analysis of the magnetism of β-HNN revealed that the interaction between the NO group and the CH group (mode B) is negligibly small. Therefore, it is not appropriate to assign the magnetic coupling, $J/k_{\mathrm{B}} = -11$ K, to the mode B. In other words, the hydrogen bonding is not relevant in the magnetic coupling in the present case. We conclude that mode A is responsible for the antiferromagnetic coupling, in spite of the short contacts between the central carbon atoms and the NO groups. According to McConnell's proposal,[9] the interactions between the carbon atom with negative spin density and the NO group with positive spin density are expected to cause ferromagnetic interactions. In our case, however, the antiferromagnetic interactions between the NO groups are considered to exceed the ferromagnetic interactions between the carbon atoms and the NO groups. Therefore, we should be careful in referring to McConnell's proposal.

BrNN and INN

BrNN and INN are isomorphous. Figure 5 shows the crystal structure of INN. Chain structure is formed along the a-axis by the a-glide reflection symmetry (I$\cdots$O distance, 2.928(3) Å is remarkably shorter than the sum of the van der Waals radii).

Dimeric structure (molecules i and ii), similar to the mode A in α-HNN, bridges the adjacent chains. The system thus becomes two-dimensional.

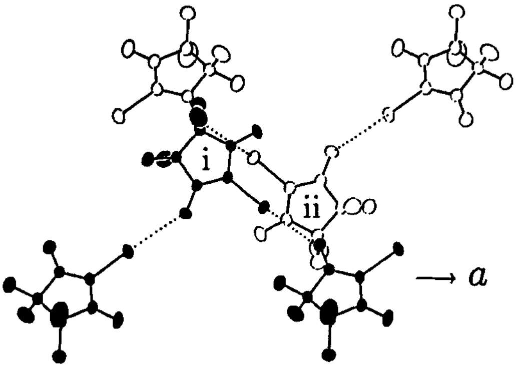

FIGURE 5 Crystal structure of INN viewed along the direction perpendicular to the ONCNO plane of molecule i.

Molecular packing of BrNN is almost the same as that of INN, whereas intrachain Br···O distance is longer (2.970(3) Å) in spite of the smaller size of the Br atom.

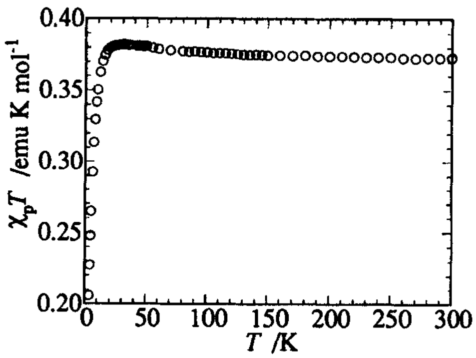

FIGURE 6 Temperature dependence of χ_pT of INN.

The χ_p's of BrNN and INN above 150 K obey the Curie-Weiss law with the Weiss constants, $\theta = -2$ K and 5 K, respectively. This indicates that the dominant magnetic interactions in BrNN and INN are antiferromagnetic and ferromagnetic, respectively. The existence of ferromagnetic interactions in INN is shown also by the plot of χ_pT against T (Figure 6); χ_pT increases as temperature lowers down to about 20 K. However, the decrease in χ_pT below about 20 K means that additional antiferromagnetic interactions also exist. Although BrNN and INN have almost the same molecular packings, the signs of dominant magnetic couplings are different.

ACKNOWLEDGMENTS

The authors are indebted to Professor Tsuneaki Goto and Dr. Hiroko Aruga Katori for the high-field magnetization measurements. This work was in part supported by the Grant-in-Aid for Scientific Research on Priority Area 'Molecular Magnetism'(Area No. 228/04242103), from the Ministry of Education, Science and Culture, Japan. Support from the New Energy and Industrial Technology Development Organization (NEDO) is also acknowledged.

REFERENCES

1 Y. Nakazawa, M. Tamura, N. Shirakawa, D. Shiomi, M. Takahashi, M. Kinoshita and M. Ishikawa, Phys. Rev. B, 46, 8906 (1992).
2 M. Tamura, Y. Nakazawa, D. Shiomi, K. Nozawa, Y. Hosokoshi, M. Ishikawa, M. Takahashi and M. Kinoshita, Chem. Phys. Lett., 186, 401 (1991).
3 M. Tamura, D. Shiomi, Y. Hosokoshi, N. Iwasawa, K. Nozawa, M. Kinoshita, H. Sawa and R. Kato, Mol. Cryst. Liq. Cryst., 232, 45 (1993).
4 Y. Hosokoshi, M. Tamura, D. Shiomi, N. Iwasawa, K. Nozawa, M .Kinoshita, H. A. Katori, T. Goto, Physica B, in press.
5 Y. Hosokoshi, M. Tamura, M. Kinoshita, H. Sawa, R. Kato, Y. Fujiwara and Y. Ueda, J. Mater. Chem., 4, 1219 (1994).
6 Y. Hosokoshi, M. Tamura, H. Sawa, R. Kato, M .Kinoshita, J. Mat. Chem., in press.
7 E. F. Ullman, J. H. Osiecki, D. G. B. Boocock and R. Darcy, J. Am. Chem. Soc., 94, 7049 (1972)
8 R. R. Gupta, Landolt-Börnstein, ed. by K. H. Hellwege and A. M. Hellwege, Springer, Berlin (1986), New Series Vol.II/16, p.3.
9 H. M. McConnell, J. Chem. Phys., 39, 1910 (1963).